



Depósito de Investigación de la Universidad de Sevilla

<https://idus.us.es/>

This is an Accepted Manuscript of an article published by Taylor & Francis in
Composite Interfaces, Vol. 22, n. 8, on 2015,
available at: <http://dx.doi.org/10.1080/09276440.2015.1056687>

FAILURE INITIATION CRITERION IN BONDED JOINTS WITH COMPOSITES BASED ON SINGULARITY PARAMETERS AND PRACTICAL PROCEDURE FOR DESIGN PURPOSES

A. Soler, A. Barroso*, V. Mantič, F. París

Group of Elasticity and Strength of Materials, School of Engineering, University of Seville, Camino de los Descubrimientos s/n, 41092, Sevilla, Spain.

* Corresponding author: abc@us.es

Keywords: composite materials, adhesively bonded joints, stress singularities, failure criteria, generalized stress intensity factors.

Abstract: Composite to metal adhesively bonded joints generates critical points where geometry and material properties change abruptly. These points (multimaterial corners) are potential locations for failure initiation. There exist proposals predicting the initiation of failure at these multimaterial corners using a Fracture Mechanics approach, in which the Generalized Stress Intensity Factors (GSIFs) at the multimaterial corner control the failure initiation. The calculation of these GSIFs at anisotropic multimaterial corners involves not-straightforward calculations of the stress singularities and characteristic angular functions, numerical modelling of the joint and a careful postprocessing of the results. In this study a parametric Finite Element Analysis has been carried out allowing the generation of plots to calculate the GSIFs for unit values of the axial force, shear force and bending moment at one end of the overlap length. These results allow calculating the GSIFs at the multimaterial corners by a simply beam analysis of the joint, the use of these plots and the application of the

superposition principle, for their use in the prediction of failure initiation by means of the singular parameters of the joint. Additionally, experiments have been carried out to propose an explicit failure criterion based on GSIF and Generalized Fracture Toughness values which fits very well with double-lap joint test results

1.- Introduction

The prediction of the failure initiation of an adhesively bonded joint with composite materials is a difficult task. Since the 40's (Volkersen [1], de Bruyne [2], Goland and Reissner [3]) and with major improvements in the 70's (Hart-Smith [4]) there are analytical tools available to predict the nominal stresses along the overlap of the bonded joint. Once the stresses can be calculated, a failure criteria can be proposed using any of the calculated variables (stresses, strains, energy,...) and comparing it with an allowable value obtained by experiments.

In the last decades, several approaches of failure proposals in adhesive joints have been addressed. Some of them based [4] on nominal values, understanding nominal as those not taking into account the local details of the joints. These local details, which include abrupt changes in material properties and geometry, give rise to singular stresses in these so-called multimaterial corners (see Figure 1), when performing a linear elastic analysis of the problem. The presence of these critical points, have also motivated the proposals of failure criteria based on the singularity parameters of the corner (Hatori [5], Groth[6]). Some proposals have also tried to obtain the nominal strength at these bimaterial corners removing the stress singularity field (Lauke and Barroso [7]), or using Cohesive Zone Models (CZM), see Mubashar et al [8] or Campilho et al. [9].

The authors of the present study have found promising evidences which support the fact that the singular stress state developed at these multimaterial corners significantly influence the failure initiation and progression in adhesive joints. These evidences cover a wide range related topics. A detailed stress characterization of the singular stress state at these corners has been obtained, including semianalytical tools to obtain the stress singularity orders and the characteristic angular functions [10] as well as numerical procedures to evaluate the Generalized Stress Intensity Factors (GSIFs) [11]. A new test, to experimentally evaluate the Generalized Fracture Toughness of pure modes in the singular stress field of the corner, has been proposed [12,13]. Many collateral aspects, such as plasticity effects, fatigue, and temperature effects giving rise to curing residual stresses have also been analyzed by the authors of this study. A comprehensive review can be found at [14]

A failure envelope was obtained [13] to predict failure in adhesively bonded joints using the GSIFs as input variables. This failure envelope covered all mode mixities, the complete K_I - K_{II} space. Nevertheless, in the framework of single- and double-lap joints subjected to tension, it has been observed that the potential combinations of K_I - K_{II} pairs fall in a very narrow area of the whole K_I - K_{II} space. That is the reason why, in this study, as a first objective, an additional experimental program was carried out to have more test in the area of interest. These tests have allowed an explicit failure criterion to be proposed in terms of the GSIFs and their allowable values (the Generalized Fracture Toughnesses).

The main drawback of a failure proposal based on singularity parameters, from a design point of view, is the necessity of making complex calculations (for the stress

singularity orders and angular shape functions) and the need of using numerical models and tedious postprocessing of results (for the GSIFs calculation). Thus, the second objective of the present study is to facilitate the design process, making a parametric analysis of different configurations, evaluating the singularity parameters (the GSIFs) and presenting them in graphical form. All complex tools, necessary to obtain the GSIFs will be fully applied to produce the plots and then, alternative geometrical configuration can be approximated by means of a simple structural analysis, the use of the superposition principle and the interpolation of the results in these plots.

2.- Tests and failure criteria

In [13] an envelope for predicting failure initiation was obtained in terms of singularity parameters K_I and K_{II} , the GSIFs of the asymptotic stress field. In particular, the failure was assumed to initiate in the bimaterial corner “c” (see Figure 1) at the end of the overlap region. This failure envelope, schematized in Figure 2, is quite general, as all mode mixities (combinations of values of K_I and K_{II}) were analyzed and experimentally determined. It was also noticed in [13] that double-lap joints in tension, with different geometrical configurations (overlap lengths, thickness, stacking sequences, etc.) presented pairs (K_I, K_{II}) in a very narrow area of the K_I - K_{II} space (see shaded area in Figure 2). It is well known that while stress singularity orders and angular shape functions only depend on the local geometry and material constants of the corner, GSIFs do depend on the global geometry and loading, nevertheless realistic changes in the geometrical configuration of the double-lap joint, slightly affects the values of the GSIFs at the critical bimaterial corner under study.

In order to give an explicit expression for the failure initiation criterion, it is clear that more tests were needed in the area of interest, namely, the third quadrant in Figure 2. The pairs (K_I, K_{II}) calculated from the real double-lap joint specimens fall in an area where the experimentally determined failure envelope had few data. These tests, described in detail in [12,13] consist on a modified configuration of the Brazilian test, in which the bimaterial corner is tested in compression at different radial orientations (Figure 3). Particularly, the third quadrant corresponds to tests in which the compression angle falls between $\alpha=115^\circ$ and $\alpha=143^\circ$, the only intermediate point, in [13], being $\alpha=120^\circ$. Tests of double-lap joints tested in shear by tension fall, for all the geometrical parameter combinations tested, between $\alpha=125^\circ$ and $\alpha=130^\circ$.

For a correct alignment of the sample, two small flat surfaces perpendicular to the load direction are slightly machined at the two contact points in the compression test. This, makes the positioning of the sample to be more stable in the loading process and the load orientation to be quite correct.

Samples for testing were manufactured in an autoclave using, for the 90° composite sector, an already cured unidirectional laminate of carbon fiber and for the 270° adhesive sector, several layers of adhesive to get the same thickness using vacuum-assisted compaction. Final disk shape was obtained by appropriate machining, always using water to avoid excessive heating and adhesive degradation. Details of samples manufacturing are equal to that used in [13], thus, full manufacturing details will be omitted for the sake of brevity.

Figure 4 shows the a) lamination of samples, b) preparation for curing, square specimens after autoclave curing and d) final circular machining for compression tests.

The mechanical properties of the materials are: unidirectional fibre laminate $[0]_{12}$, $E_{11}=141300$ MPa, $E_{22}=E_{33}= 9580$ MPa, $\nu_{12}=\nu_{13}=0.3$, $\nu_{23}=0.32$, $G_{23}=3500$ MPa, $G_{12}=G_{13}=5000$ MPa for CFRP AS4/8552 (1 being the fibre direction) and $E=3000$ MPa, $\nu=0.35$ for the adhesive FM[®]73 OST (toughened epoxy film, from Cytec). For the aluminum used in the double-lap joints specimens, a 2024-T3 has been used with $E=68670$ MPa and $\nu = 0.33$.

The procedure to generate the failure envelope consisted in testing the Brazilian disk specimens corresponding to the load orientations ($115^\circ < \alpha < 145^\circ$) giving rise to a quite reasonable density of (K_I, K_{II}) values falling in the third quadrant. Numerical modellization of each sample was carried out using a Finite Element model, and GSIF values (K_I, K_{II}) were calculated at the experimental failure load. Figure 5 shows the tests results obtained, with two samples at $\alpha=115^\circ$ and $\alpha=145^\circ$ (for comparison purposes with the previous experimental results in [13]) and three samples for each intermediate load angle (each 5°).

The test results for the Brazilian disk specimens (circular dots) have been used to perform a least squares fitting with the proposed failure criterion in (1) in which an exponential interaction between the two terms (K_I and K_{II}) is proposed and the exponent n is fitted. The failure proposal has been non-dimensionalized with the corresponding Generalized Fracture Toughness values K_{IC} and K_{IIC} due to the fact that each GSIF (K_I and K_{II}) have different dimensions.

$$\left(\frac{K_I}{K_{IC}} \right)^n + \left(\frac{K_{II}}{K_{IIC}} \right)^n \leq 1 \quad (1)$$

Equation (1) is a proposal for failure initiation. Results for failure initiation taken into account for Figure 5 were defined in most of the cases when some initial defect was visible at the corner, but no catastrophic failure produced in the sample.

In Figure 5, three values of the exponent n , in (1), have been plotted. The straight line in green corresponds to $n=1$, the red circumference corresponds to $n=2$. The brown curve corresponds to the best value, in terms of least squares, of expression (1) and corresponds to $n=1.6$.

A simple and safe failure criterion for failure initiation is proposed taking $n=1$, leaving a certain safety factor which depends on the mixity of the GSIF values.

Figure 5, and equation (1) represents a reliable failure initiation proposal for adhesively bonded lap joints having the last ply of the laminate, in contact with the adhesive layer, at 0° (which is the bimaterial closed corner covered in the present study). Other fiber orientations of the last ply in contact with the adhesive layer can be calculated by just repeating the tests and the numerical modelling (of the Brazilian disk specimen), to define a new failure curve.

Nevertheless, although a failure curve can be obtained as proposed in the present study, its use in design is not straightforward due to the fact that the calculation of GSIF values for a particular geometry is not simple. It involves detailed numerical modelling of the structure and a careful postprocessing of the results.

Next section is a step forward helping engineers to use the proposed failure criteria based on singular parameters of the stress state (the GSIFs) but without the cumbersome part of the calculations.

3.- Practical application for design, parametric study

3.1.- Parameters taken into account

As mentioned in previously, the complete procedure to fully characterize the singular stress field in a multimaterial corner with composite materials is not easy and several complex steps are involved in the calculations. All these tools are available in literature, but it is neither realistic nor practical for designers to use them. Thus, to try to overcome these difficulties, a parametric study has been carried out varying some geometrical and mechanical parameters defining the joint.

Due to the particular geometry of these types of joints, typically joining thin laminates with geometry and loading not varying along the bond line, GSIF values have been obtained for unitary load cases (axial force, shear force and bending moment) which have been applied at one end of the joint at a normalized distance of one overlap length and assuming a generalized plane strain state. GSIFs (K_I and K_{II}) defining the singular stress field at the critical corner under study have been calculated following the procedure proposed in [11] which consists on a least squares fitting of displacement (and/or stress values) evaluated at the neighborhood of the corner by means of a Finite Element model with a fine mesh at the corner tip. This unitary load cases have been applied to single- as well as to double-lap joints.

For these unitary load cases in both configurations (single- and double-lap), three parameters have been analyzed.

a) The thickness (e) of the reference adherent, with $e=1$ mm and 4 mm. Notice that in a joint of dissimilar materials (composite to metal), a balanced joint (that having equal total axial stiffness $e_1 \cdot E_1 = e_2 \cdot E_2$) typically implies different thickness values. Thus, the thickness of one of the adherents (e_1 or e_2) has to be taken as the reference thickness value (e).

b) The overlap length to thickness ratio (L/e) with $L/e=10, 50, 100$. This parameter is non-dimensional.

c) The balance factor of the joint (d) measured as the ratio of total axial stiffness of each adherent, $d = E_1 \cdot e_1 / E_2 \cdot e_2$ for single-lap joints and $d = 2 \cdot E_1 \cdot e_1 / E_2 \cdot e_2$ for double-lap joints (subindex "1" denoting the outer adherent). This parameter is also non-dimensional and takes, in this parametric analysis, values of $d=0.5, 1$ (balanced), 2.

Three unitary loading cases (axial force N , shear force V and bending moment M) were applied to each one of the combinations at one overlap length from the overlap end of the joint, for both single-lap "SL" and double-lap "DL" joint geometries.

A total of 108 models were analyzed $(3 L/e) \times (2 e) \times (3 d) \times (N,V,M) \times (SL,DL)$.

Once all these cases are numerically computed, any other load and geometrical configuration can be estimated by interpolating the previous results. For that end, the superposition principle is being used under the assumption of a linear elastic state of the joint.

3.2.- GSIF's plots

Once all these cases are numerically computed, any other load and geometrical configuration can be estimated by interpolating the previous results. For that end, the superposition principle is being used under the assumption of a linear elastic state of

the joint. The results of the parametric analysis are summarized in three plots, one for each unitary loading case, and are presented in figures 11 (axial load), 12 (shear load) and 13 (bending moment).

In figures 11-13, the legend in the top part of the figures gets the form: $K_{\#}(e\#-d\#)$, where $\#$ are numbers. The number following the “K” denoting the GSIF component, the number following the “e” denoting the thickness (in mm) and the number following the “d” denoting the dimensionless imbalance factor ($d=0.5, 1, 2$). The vertical axes show K_1 (left-hand axis) and K_2 (right-hand axis) values respectively, while the horizontal axis show the non-dimensional overlap vs thickness ratio (L/e).

The values considered for each one of the parameters is wide enough for results in figures 11-13 to be useful for many real joint configurations. Also, the observed variations of K_I and K_{II} are quite smooth so that interpolations are expected to be a good estimation of the real values of the GSIFs.

Results for the axial force case (Fig. 11) and bending moment case (Fig. 13) show almost no influence with respect to the L/e (overlap length to thickness ratio).

Nevertheless, results for the shear force are sensitive to this parameter. Recall that the unit (axial/shear) load or the bending moment are applied at a distance of the overlap end equal to one overlap distance. Thus, the same unit shear load has a greater moment arm when L/e increases, no significant change being generated in the loading configuration of the joint for the axial load or bending moment.

Any conclusion or trend made from results in figures 11-13 have to take into account that the load or bending moment is always unitary. Thus, for example, if the thickness

of the adherents increases, the nominal normal tensile stresses will decrease in the axial loading case. If results for K_I and K_{II} are equal for both values of the thickness, it should be concluded that for equal stress values, K_I and K_{II} values will be greater in the case of greater thickness.

With this fact in mind, some clear trends can be observed. For example, in Figure 12, all K_I and K_{II} values are lower as thickness increases from 1 mm (e_1) to 4 mm (e_4). The same trend is observed in figure 13. As thickness increases, the total stiffness of the joint increases and GSIF values, for the same load values, decrease consequently.

3.3.- Practical application. An example.

Figure 14 shows the scheme of a structure, with the presence of an adhesive joint. The application of the interpolation procedure proposed previously assumes a linear elastic behavior of the structure (to apply the superposition principle) and can be summarized in two simple steps.

- a) Structural analysis of the problem, using a Strength of Materials approach, to obtain the axial and shear forces and also the bending moment at a distance (L) far from one end of the overlap region of the joint (N=5, V=-2, M=4 in the example of the figure).
- b) Application of the superposition principle and use of the previously obtained plots (figures 11-13) to determine the GSIF values, as shown in equation (2).

$$K_{I,II} = 5 \cdot K_{I,II(N=1)} - 2 \cdot K_{I,II(V=1)} + 4 \cdot K_{I,II(M=1)} \quad (2)$$

Each term ($K_{I,II(N=1)}$, $K_{I,II(V=1)}$, $K_{I,II(M=1)}$) can be obtained from Figures 11-13 by simply calculating the (L/e) parameter, which is the x-axis value. Then, the imbalance parameter (d) has to be calculated which, together with the value of the thickness (e), will define the appropriate curve from which to obtain the K value. Values of $K_{I,II}$ corresponding to values of (d) and/or (e) not equal to those included in Figures 11-13 should be linearly interpolated from values of $K_{I,II}$ associated to values of (d) and/or (e) available in these figures.

4.- Conclusions and future developments

In the present study a procedure for predicting the initiation of failure in corner points of adhesively bonded joints has been proposed.

A failure criterion, based on critical values of the Generalized Stress Intensity Factors (GSIFs) of the multimaterial corner has been proposed. A modification of the Brazilian test has been used, with the corner in the center of the disk, to determine the allowable values of the GSIFs.

A simplified procedure to determine the GSIFs has been proposed, based on the superposition principle. A parametric analysis has been carried out to obtain the GSIFs of the critical points based on a simple structural analysis of the structure (determination of the axial load, shear load and bending moment). Unit load plots have been obtained which allow the straightforward determination (by interpolation) of the GSIFs.

The complete procedure will help designers and engineers to use the failure approach based on stress singularities without the necessity of performing complex calculations and also avoiding the necessity of numerical models of the corner configuration.

References

- [1] Volkersen O. Die Niekraftverteilung in Zugbeanspruchten mit Konstanten Laschenquerschnitten. Luftfahrtforschung 1938;15: 41-47.
- [2] De Bruyne NA. The strength of glued joints. Aircraft Eng. 1944;16:115-118.
- [3] Goland M, Reissner E. The stresses in cemented joints. J. Appl. Mech. 1944;11: A17-A27.
- [4] Hart-Smith LJ. Analysis and design of advanced composite bonded joints. NASA CR-2218, 1974.
- [5] Hattori TA. Stress-singularity-parameter approach for evaluating the adhesive strength of single lap joints. JSME Int. J. I-Solid M. 1991;34: 326-331.
- [6] Groth HL. Stress singularities and fracture at interface corners in bonded joints. Int. J. Adhes. Adhes. 1988;8:107-113.
- [7] Lauke B, Barroso A. Notched-Butt Test for the Determination of Adhesion Strength at Bimaterial Interfaces. Compos. Interface. 2011;18:661–669.
- [8] Mubashar A, Ashcroft IA, Critchlow GW, Crocombe AD. Strength prediction of adhesive joints after cyclic moisture conditioning using a cohesive zone model. Eng. Fract. Mech. 2011;78:2746-2760.
- [9] Campilho RDSG, Banea MD, Neto JABP, Da Silva LFM. Modelling adhesive joints with cohesive zone models: Effect of the cohesive law shape of the adhesive layer. Int. J. Adhes. Adhes. 2013;44:48-56.
- [10] Barroso A, Mantič V, París F. Singularity analysis of anisotropic multimaterial corners. Int. J. Fracture. 2003;119:1-23.

- [11] Barroso A, Graciani E, Mantič V, París F. A least squares procedure for the evaluation of multiple generalized stress intensity factors at 2D multimaterial corners by BEM. *Eng. Anal. Bound. Elem.* 2012;36:458-470.
- [12] Barroso A, Vicentini D, Mantič V, París F. Generalized fracture toughness determination in multimaterial closed corners with two singular terms. Part I: Test proposal and numerical analysis. *Eng. Fract. Mech.* 2012;89:1-14.
- [13] Vicentini D, Barroso A, Justo J, Mantič V, París F. Generalized fracture toughness determination in multimaterial closed corners with two singular terms. Part II: Experimental results. *Eng. Fract. Mech.* 2012;89:15-23.
- [14] Mantič V, Barroso A, París F. Singular elastic solutions at anisotropic multimaterial corners. Applications in composites. In Mantič V, editor, *Mathematical Methods and Models in Composites*. 2014:425-496. Imperial College Press, London.

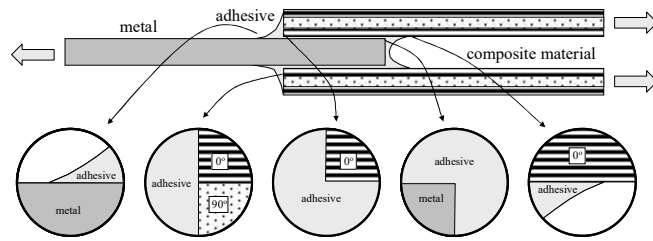


Figure 1.- Corner points in an adhesively bonded joint.

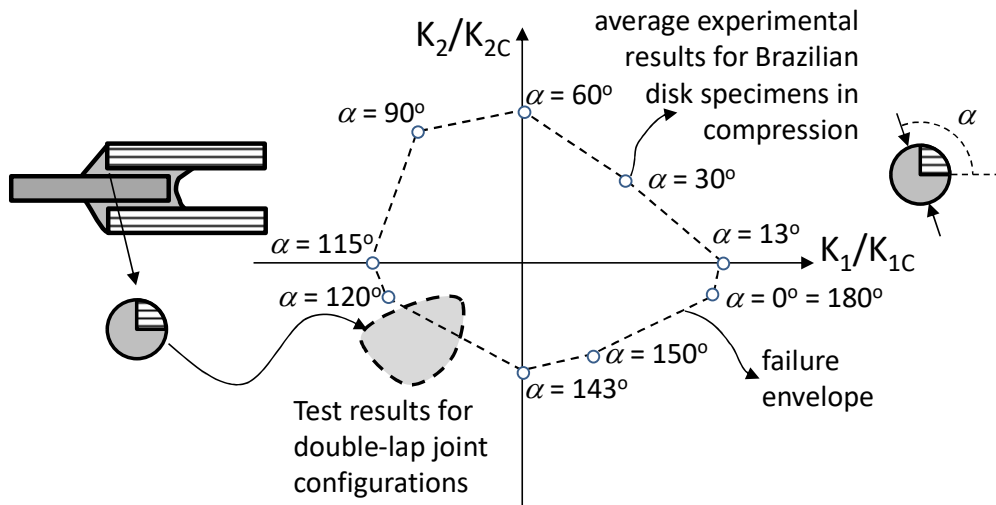


Figure 2.- Schematic representation of failure envelope and results on double-lap joints.



Figure 3.- Test of one specimen containing the bimaterial corner in compression to obtain the failure envelope.

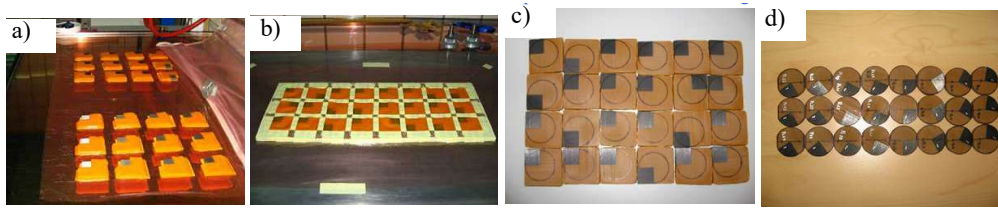


Figure 4.- Preparation of Brazilian disk samples of the bimaterial corner.

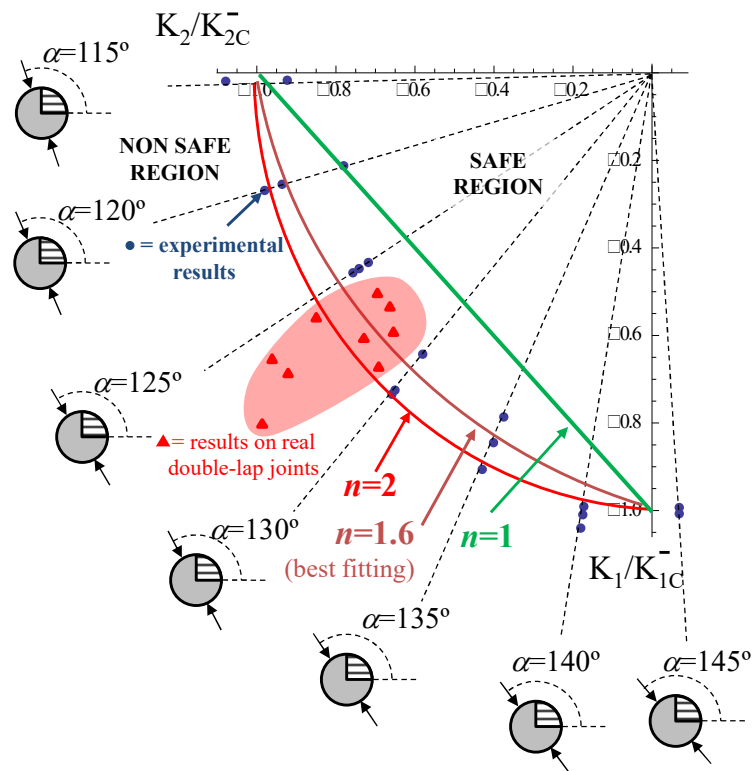


Figure 5.- Result of the Brazilian tests and suggested failure envelopes.

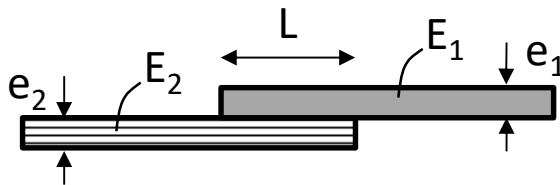


Figure 6.- Joint parameters included in the analysis.

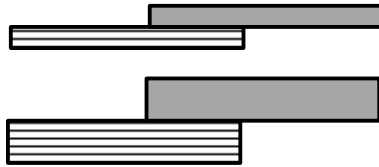


Figure 7.- Effect of thickness in the GSIF's calculation.

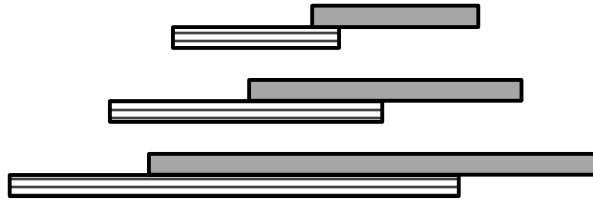


Figure 8.- Effect of overlap length in the GSIF's calculation.

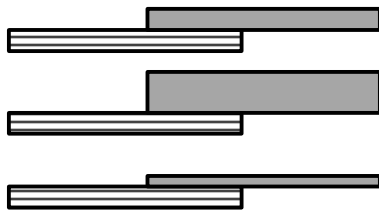


Figure 9.- Effect of imbalance in the GSIF's calculation.

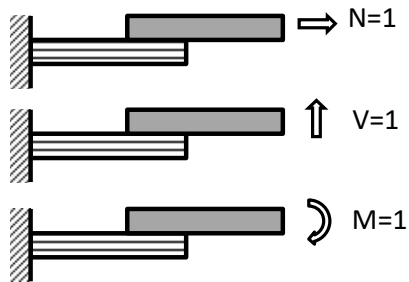


Figure 10.- Unitary load cases of the analysis.

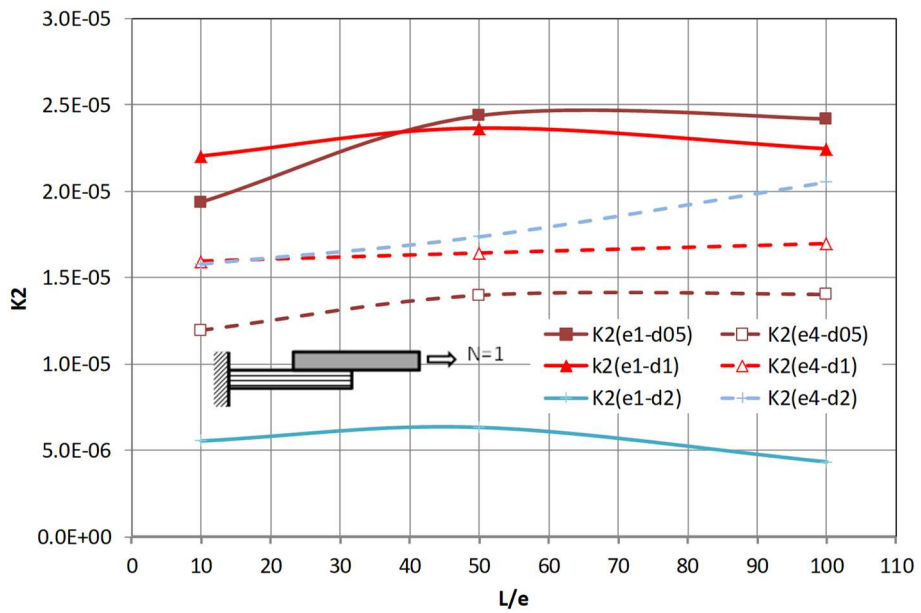
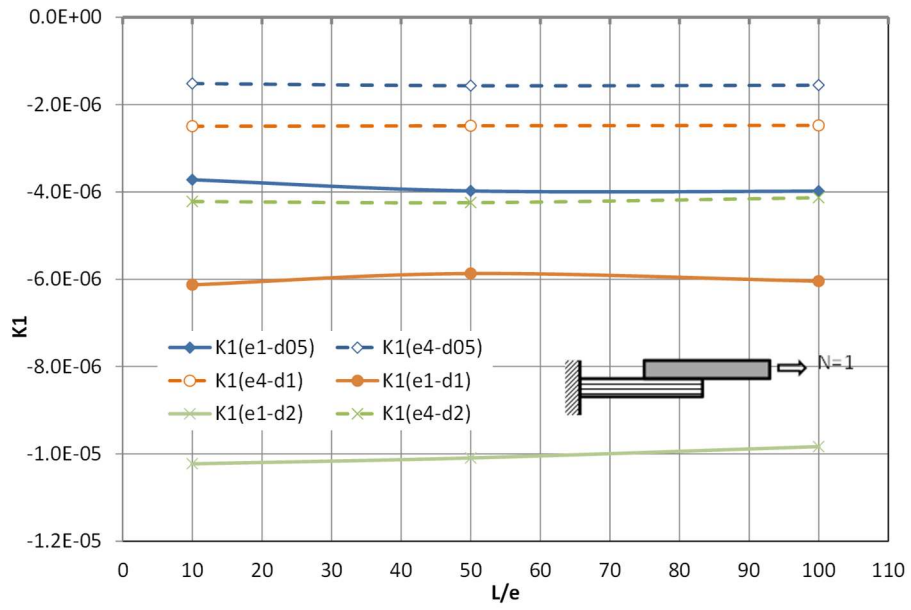


Figure 11.- Results for GSIFs (K_1 , K_2) for the unit axial load case.

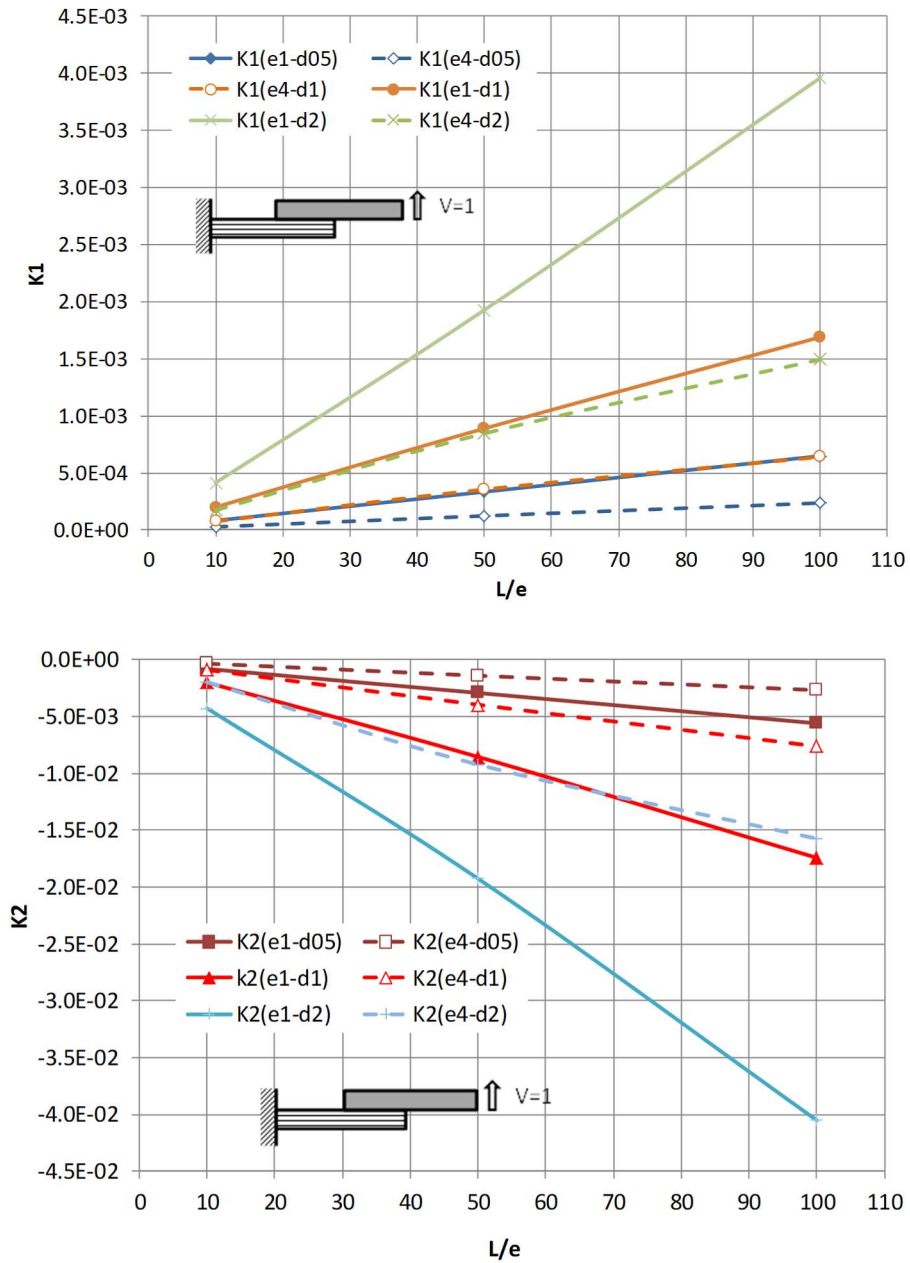


Figure 12.- Results for GSIFs (K_1 , K_2) for the unit shear load case.

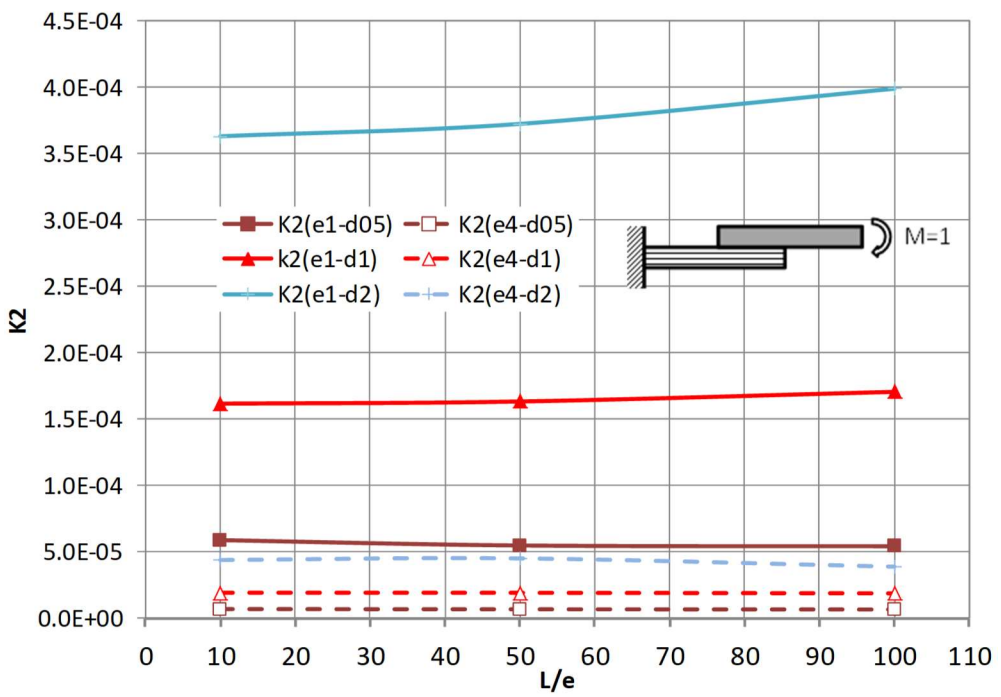
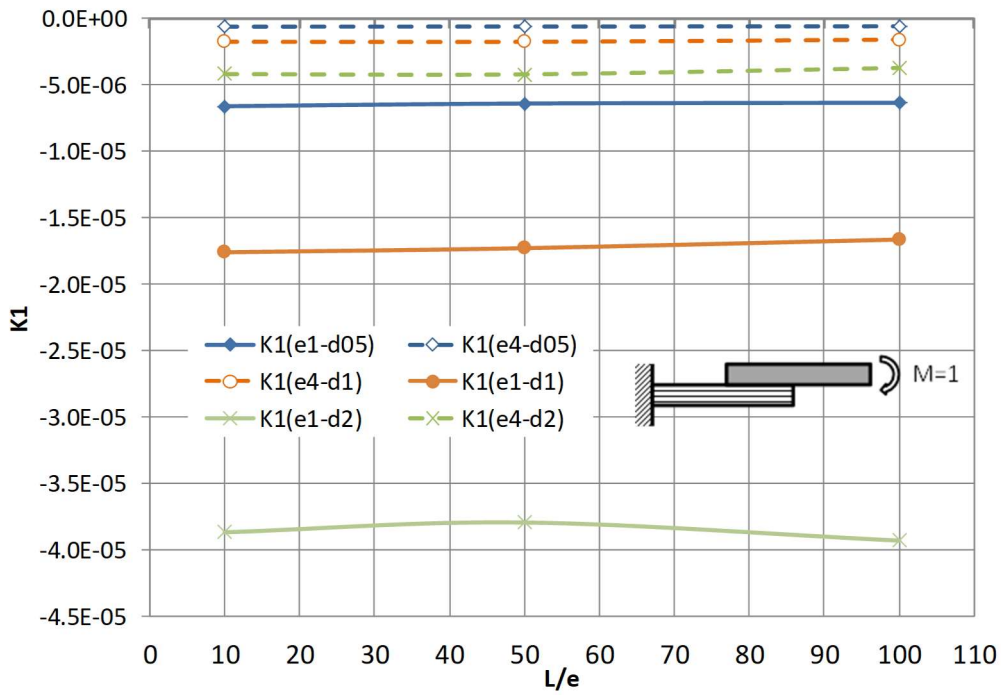


Figure 13. Results for GSIFs (K_1 , K_2) for the unit bending moment load case.

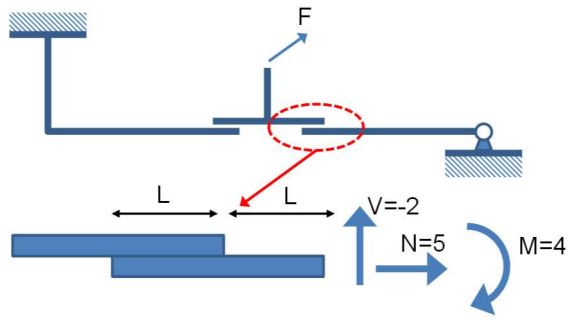


Figure 14. Example of a real structure, application of the procedure.